

RESEARCH ARTICLE

10.1002/2017JD026592

Key Points:

- Midtropospheric warming in the Peruvian Andes is destroying climate signals preserved in glaciers and driving glacier retreat
- The impact of the 2015/2016 El Niño on Quelccaya ice cap was more pronounced than for previous events in the last four decades
- Peruvian Andes snow $\delta^{18}\text{O}$ is linked to tropical Pacific SSTs, regional 500 mb temperatures, and convection

Supporting Information:

- Supporting Information S1

Correspondence to:

L. G. Thompson,
thompson.3@osu.edu

Citation:

Thompson, L. G., Davis, M. E., Mosley-Thompson, E., Beaudon, E., Porter, S. E., Kutuzov, S., ... Mountain, K. R. (2017). Impacts of recent warming and the 2015/2016 El Niño on tropical Peruvian ice fields. *Journal of Geophysical Research: Atmospheres*, 122, 12,688–12,701. <https://doi.org/10.1002/2017JD026592>

Received 3 FEB 2017








Accepted 6 SEP 2017

Accepted article online 17 SEP 2017

Published online 11 DEC 2017

©2017. American Geophysical Union.
All Rights Reserved.

Impacts of Recent Warming and the 2015/2016 El Niño on Tropical Peruvian Ice Fields

L. G. Thompson^{1,2} , M. E. Davis¹ , E. Mosley-Thompson^{1,3} , E. Beaudon¹ , S. E. Porter¹ , S. Kutuzov⁴ , P.-N. Lin¹ , V. N. Mikhailenko⁴, and K. R. Mountain⁵

¹Byrd Polar and Climate Research Center, The Ohio State University, Columbus, OH, USA, ²School of Earth Sciences, The Ohio State University, Columbus, OH, USA, ³Department of Geography, The Ohio State University, Columbus, OH, USA, ⁴Institute of Geography, Russian Academy of Sciences, Moscow, Russia, ⁵Department of Geography and Geosciences, University of Louisville, Louisville, KY, USA

Abstract Data collected between 1974 and 2016 from snow pits and core samples from two Peruvian ice fields demonstrate the effect of the recent warming over the tropical Andes, augmented by El Niño, on the preservation of the climate record. As the 0°C isotherm is approaching the summit of the Quelccaya ice cap in the Andes of southern Peru (5,670 meters above sea level (masl)), the distinctive seasonal $\delta^{18}\text{O}$ oscillations in the fresh snow deposited within each thermal year are attenuated at depth due to melting and percolation through the firn. This has become increasingly pronounced over 43 years. In the Andes of northern Peru, the ice field on the col of Nevado Huascarán (6050 masl) has retained its seasonal $\delta^{18}\text{O}$ variations at depth due to its higher elevation. During the 2015/2016 El Niño, snow on Quelccaya and Huascarán was isotopically ($\delta^{18}\text{O}$) enriched and the net sum of accumulation over the previous year (NSA) was below the mean for non-El Niño years, particularly on Quelccaya (up to 64% below the mean) which was more pronounced than the NSA decrease during the comparable 1982/1983 El Niño. Interannual large-scale oceanic and middle to upper-level atmospheric temperatures influence $\delta^{18}\text{O}$ in precipitation on both ice fields, although the influences are variably affected by strong El Niño–Southern Oscillation events, especially on Quelccaya. The rate of ice wastage along Quelccaya’s margin was dramatically higher during 2015/2016 compared with that of the previous 15 years, suggesting that warming from future El Niños may accelerate mass loss on Peruvian glaciers.

1. Introduction

Evidence is mounting that the rate of tropospheric warming is increasing with elevation due to factors such as latent heat release, atmospheric aerosol loading, and feedbacks involving albedo, water vapor, and radiation fluxes (Pepin et al., 2015). The current warming has resulted in more negative mass balances on many tropical ice caps and glaciers. Several recent studies document that glacier melting is well underway in the tropics, and that many glaciers in the tropical Andes are diminishing at faster rates than at any time since the middle of the Little Ice Age (Francou et al., 2003; Thompson et al., 1993, 2013) and slightly faster than glacier retreat on a global scale (Rabatel et al., 2013). The most rapid rate of retreat has occurred in the last 50 years (Rabatel et al., 2013), and many small, low-elevation glaciers in the tropical Andes are projected to disappear within a few decades (Rabatel et al., 2013; Schauwecker et al., 2014; Vuille, Francou, et al., 2008). During the twentieth century, precipitation has not shown a consistent trend and therefore is not considered to be the primary factor driving the ice retreat (Rabatel et al., 2013). However, a warming trend in atmospheric temperature ($\sim 0.10^\circ\text{C}/\text{decade}$ in the last 50 years) has been observed over glaciers in the central Andes (Bradley et al., 2009) and this, in addition to the intensity of major El Niño events, is most likely a dominant forcing for the recent wasting (Hanshaw & Bookhagen, 2014; Perry et al., 2014; Vuille, Francou, et al., 2008). Future warming is projected to be greater at higher altitudes, potentially increasing at least 4°C by the end of the 21st century (Bradley et al., 2006; Urrutia & Vuille, 2009).

The majority of the precipitation in the central and southern Peruvian Andes and Altiplano falls during the austral summer (December to February, or DJF) (Garreaud et al., 2003; Mantas et al., 2015) in association with the South American summer monsoon (SASM). The intensity of the SASM is influenced by convection enhanced by a deep low-pressure system that forms in the summer over the Chaco region (eastern Bolivia, western Paraguay, and northern Argentina). The latent heat from the convection contributes to the formation of the Bolivian High, a persistent upper-level high-pressure system over the Bolivian Altiplano and

southeastern Amazon Basin (Lenters & Cook, 1997). Anticyclonic circulation associated with the Bolivian High results in upper- and middle-level easterly to northerly transport of moist air to the Andes and Altiplano which strengthens deep convection over this region (Garreaud et al., 2003, 2009). The negative southern oscillation phase of the El Niño–Southern Oscillation (ENSO), which occurs during El Niño, has a strong influence over moisture transport from the Amazon to the Andes, partly through strengthened westerly air flow over the central Andes which inhibits low- and middle-level easterly flow from the northern Amazon Basin during the austral summer (Garreaud & Aceituno, 2001; Vuille et al., 2000). Strong El Niños are also responsible for anomalous warming of up to 4°C in the middle troposphere in the tropics, which has significant impacts on freezing level heights (Diaz et al., 2014).

Snow layers deposited on tropical Andean glaciers during austral summer are isotopically depleted relative to winter layers (June to August) (Hurley et al., 2015; Thompson, 1980). Sublimation and water vapor diffusion through the surface snow are thought to promote ^{18}O enrichment during the dry season (Hurley et al., 2015) when little fresh snow is deposited. In addition, snowfall amounts on seasonal to decadal timescales can be influenced by tropical atmospheric and oceanic processes (Garreaud et al., 2003; Hurley et al., 2015; Thompson et al., 2013; Vuille et al., 2000). However, **the interpretation of stable isotopic ratios of oxygen ($\delta^{18}\text{O}$) and hydrogen (δD) in the precipitation has been controversial, especially with regard to the influence of air temperature versus precipitation amount.** Early studies (Dansgaard, 1964; Rozanski et al., 1993) indicate that for tropical rainfall, precipitation amount is the more important influence on stable isotopic ratios. However, other atmospheric and oceanic processes undoubtedly affect isotopic ratios to varying degrees. In the tropical Andes these include air mass stability over the Amazon (Grootes et al., 1989), tropical Pacific sea surface temperatures (Bradley et al., 2003; Thompson et al., 2011, 2013), ENSO-related atmospheric circulation (Bradley et al., 2003; Henderson et al., 1999; Vuille et al., 2000, 2003), and South American summer monsoon dynamics (Hurley et al., 2015). Specifically, Hurley et al. (2015) proposed that snowfall amount, which is at its maximum during DJF and is enhanced by cold air incursions from higher latitudes, is the driver of the isotopic ratios. Recent studies of tropical precipitation, however, conclude that convection-associated condensation temperature is a major influence (Cai & Tian, 2016; Permana et al., 2016; Scholl et al., 2009).

The Quelccaya ice cap (QIC, 13.9°S; 70.8°W; 5,670 meters above sea level, or masl), the world's largest tropical ice cap, is located on the northern edge of the Altiplano in the Cordillera Vilcanota, one of the easternmost ranges of the Andes of southern Peru (Figure 1). To the north, Earth's highest tropical mountain, Nevado Huascarán (HS, 9.1°S; 77.6°W; 6768 masl at the highest peak) in the Cordillera Blanca of central Peru is located 200 km from the western edge of the Amazon Basin. Both sites have high snow accumulation rates (~2 to 3 m/yr) and, until very recently on the QIC, minimal reworking of the surface snow during the austral summer. The ice on HS retains distinct seasonal layers in dust and $\delta^{18}\text{O}$ which have been used to reconstruct annually resolved records of environmental and climatic variations back to 1720 Common Era (C.E.). The complete record from a deep core drilled on HS in 1993 extends back 19,000 years (Thompson et al., 1995). On Quelccaya the seasonal variations in $\delta^{18}\text{O}$ are greatly attenuated in the latter half of the twentieth century record, although the seasonality in mineral dust is preserved. Annually resolved climate records which extend back 1,500 to 1,800 years were recovered from the QIC in 1983 and 2003, respectively (Thompson et al., 1985, 2013). Surface sampling and margin photogrammetry have been conducted on the QIC since 1974, which makes it the longest monitored tropical ice cap. Glaciological observations since the 1970s provide evidence that it has been retreating along its margins (Albert et al., 2014; Brecher & Thompson, 1993; Hanshaw & Bookhagen, 2014; Thompson et al., 1982, 2006, 2013). Ice core and geophysical data suggest that the retreat is driven by the warming environment, just as the Late Holocene fluctuations of its largest outlet glacier (Qori Kalis) were temperature driven (Stroup et al., 2014). Margin retreat is associated with seasonal elevation rise of the 0°C isotherm (freezing level height) and sporadic melting at the summit during the austral summer (Bradley et al., 2009). This trend persevered in the high elevations of the tropical Andes through the warming "hiatus" from 2000 to 2009, which is consistent with the continuous warming at higher elevations during this period (Vuille et al., 2015).

Here we present field observations and data from pits and shallow core samples collected on the summit of the QIC between 1974 and 2016, from a deep core drilled on the HS col in 1993, and from a shallow core drilled in 2016 on HS to demonstrate how the recent warming over the tropical Andes has affected the preservation of the climate records in the upper layers of these ice fields. We analyze $\delta^{18}\text{O}$ profiles and the



Figure 1. Relief map of Peru showing regions of highest elevation along the Andes Mountain Range and the locations of the Quelccaya ice cap and Nevado Huascarán ice field.

density-adjusted net sum of accumulation over the previous year prior to sampling (NSA) as defined by Hurley et al. (2015), to determine the effect that major ENSO events, particularly the 2015/2016 El Niño, have had on the QIC and HS climate records as well as on the retreat of a margin of the QIC. Finally, we provide evidence for large-scale atmospheric and oceanic influences on the $\delta^{18}\text{O}$ values in precipitation on these tropical ice fields.

2. Materials and Methods

During 24 expeditions to the QIC between 1974 and 2016, the Ice Core Paleoclimatology Research Group at The Ohio State University's Byrd Polar and Climate Research Center (BPCRC) collected shallow and deep cores and pit samples from the summit dome. In the 1970s and in 2003 lower domes on the ice cap were also drilled, although for this investigation only the summit pits and cores are used. Although this type of

long-term sampling was not conducted on HS, in 1991 a shallow core was drilled on the 6050 masl col between the northern and southern peaks and in 1993 the col was drilled to bedrock (Thompson et al., 1995). HS was not visited by BPCRC again until July of 2016, when a 10.3 m firn core was recovered from the col.

All field seasons on both ice fields were conducted during the dry austral winters. Field activities on the QIC included excavation and sampling of pits 2–3 m deep to ensure that the most recent thermal year's precipitation (austral winter to austral winter) was collected. The sampling protocols throughout the 24 expeditions were similar but not strictly consistent. During most field seasons pits were excavated and shallow cores were drilled, although on some occasions only one of these activities was undertaken (see supporting information). Only the deep cores drilled on the summit and north domes of the QIC in 2003 and one of the two deep cores drilled on HS in 1993 were transported to BPCRC intact (i.e., frozen). All samples collected during the other 23 QIC expeditions and the 1991 and 2016 expeditions to HS were individually bagged, melted, and bottled at the field sites before shipment to BPCRC.

All pit and core samples from the QIC and HS were analyzed for $\delta^{18}\text{O}$. Figure S1 in the supporting information displays $\delta^{18}\text{O}$ plots of all the summit dome pits and up to the top 16 m of the cores from the QIC, including the 2003 summit dome deep core. The lower boundary of each top thermal year (TY1) is determined by the most ^{18}O -enriched (less negative) samples that occur during the winter dry season and are supported by peaks in aerosol (mineral dust and/or major ion) concentrations where such data exist. For example, see the discussion (supporting information Text S1 and Figure S2) for the dating of the shallow cores collected in 2016 from the QIC and HS, in which dust and especially the nitrate concentrations (smoothed with three-sample running means) show wet/dry season variations that are in phase with low/high $\delta^{18}\text{O}$ values and thereby allow thermal year determinations. This is particularly important for the 2016 QIC core since the seasonal $\delta^{18}\text{O}$ signal is not distinct in TY1 and is completely smoothed below 6 m.

Hourly snow height measurements made on the surface of the QIC over 10 years, along with weather station data, show that snow accumulation peaks in December and that $\delta^{18}\text{O}$ values decrease through the SASM season (Hurley et al., 2015). In contrast, no net accumulation is observed during the austral winter and alteration of the surface by sublimation results in ^{18}O enrichment. Stichler et al. (2001) concluded from an experiment conducted on the surface of an Andean glacier (5,536 masl) that sublimation during the summer has a limited effect on the preserved isotopic record below the top several centimeters. In addition, low nocturnal temperatures promote water vapor condensation and refreezing in the near-surface firn pores, inhibiting isotopic enrichment in deeper layers. Hurley et al. (2015) found net water equivalent accumulation and net snow-height change as measured by an automated weather station (AWS) to be highly and significantly correlated at the QIC summit. The differences between pit depths and AWS-measured snow height changes between 2004/2005 and 2013/2014 are less than 10%, and usually less than 5%. Decreases in snow height are most intense from August to September, although some lowering occurs from June to July. This is attributable to postdepositional processes such as snow sublimation at the surface and densification within the TY1 firn. However, due to the timing of ablation with respect to the summit snow sampling in June–August for all 24 field seasons, except that conducted in September 1991, and the lack of large melt features within the TY1 layers, we conclude that little or no melting has occurred in the top thermal years which might have redistributed mass downward. The exception may be the 2015/2016 El Niño TY1, which is discussed below. Therefore, for the purposes of the pit and shallow core analyses, annual averages of $\delta^{18}\text{O}$, which are biased toward the wet season (Hurley et al., 2015), are assumed to represent wet season values. Although no similar meteorological monitoring has been conducted on HS, we make the same assumptions since precipitation variations (dominated by ENSO) are governed by similar, although not identical, atmospheric processes throughout the central Andes (Vuille, Kaser, et al., 2008).

3. Recent Changes in the QIC and HS Near-Surface Layers

Since the beginning of the long-term program on the QIC, several changes have been observed throughout the firn pack. To demonstrate this, the $\delta^{18}\text{O}$ profiles from several shallow cores drilled on the summit dome in 1976, 1979, 1983, 1991, and 2016 and the top of the 2003 deep core are shown in Figure 2a. With the exception of the 1983 and 2016 shallow cores which were drilled at the end of major El Niño events, the snow deposited in TY1 (shaded in gray) of each profile is generally 2 to 3 m thick and retains the characteristic

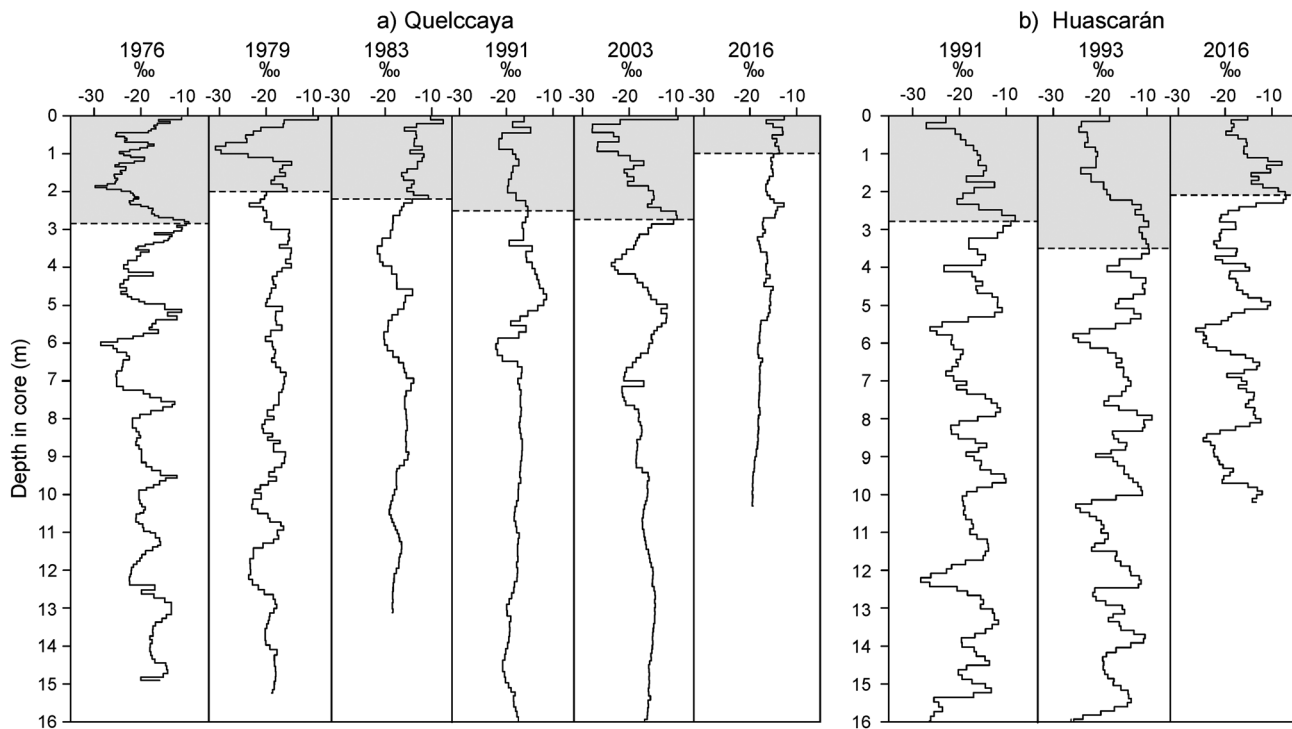


Figure 2. (a) $\delta^{18}\text{O}$ profiles from selected QIC summit cores drilled over the last four decades. (b) $\delta^{18}\text{O}$ profiles from the tops of the Huascarán 1991 shallow core, the 1993 deep core, and the entire 2016 shallow core. The top thermal years are shaded.

seasonal isotopic variations (**winter enrichment, SASM depletion**). Visible stratigraphy observed during pit excavation confirms the lack of vertical ice conduits which suggests that little or no water percolation occurred through the top of the snow/firn column during the first year of deposition and densification. However, these shallow core $\delta^{18}\text{O}$ profiles illustrate the progression over four decades of postdepositional changes at the summit of the QIC.

The 1976 record shows distinctive seasonal $\delta^{18}\text{O}$ variations preserved throughout its length, although the signal is naturally smoothed by vapor diffusion in the firn. This process weakens the expression of seasonal $\delta^{18}\text{O}$ variations at depth (Johnsen et al., 2000). By 1979, the seasonal $\delta^{18}\text{O}$ variations, although still discernible, were dampened below TY1. This attenuation of the seasonal signal progressed through the next 25 years. By 2003, when the ice cap was drilled to bedrock for the second time, the $\delta^{18}\text{O}$ oscillations were almost completely smoothed below 7 m and were absent throughout the 2016 shallow core, even within TY1. In contrast, the $\delta^{18}\text{O}$ profiles from HS show that the seasonality of the $\delta^{18}\text{O}$ signal has persisted from 1991 to 2016 (Figure 2b). Although HS is 880 km northwest of the QIC and located deeper in the tropics, the drill site on the col is 380 m higher than the summit of the QIC.

The depths to which the effects of warming over recent decades have descended through the top of the QIC, through the firn and even into the ice, are evident in the deep cores which were drilled 20 years apart. Figures 3a and 3b show the $\delta^{18}\text{O}$ stratigraphies through the upper 60 m of the 1983 summit core (dated back to 1925) and the 2003 summit dome core (dated back to 1945). The density trends (Figure 3c) of these two cores increase similarly within the top 11 m, although between ~ 11 and ~ 24 m the 2003 core appears to show a higher density trend than that in the 1983 deep core over the same depth interval. The 2003 core transitions to ice (830 kg/m^3) at ~ 18 to 19 m, but the earlier ice core reaches that density at ~ 21 to 22 m resulting in an average rise in the firn/ice transition of ~ 15 cm/yr. Melting at the summit of the QIC may have started between 1979 and 1981, since the seasonal $\delta^{18}\text{O}$ attenuation in the 1979 shallow core may have been the result of increased vapor diffusion through the firn. The shallow core drilled on the summit in 1981 contained a 15 cm section of water-soaked firn at 24.5 m depth, and during the first deep drilling program in 1983 meltwater was actually observed in a 42 cm section of firn just above the firn/ice transition at ~ 22 m. However, in 1991 the drilling at the summit by hand auger was suspended at 21.25 m when

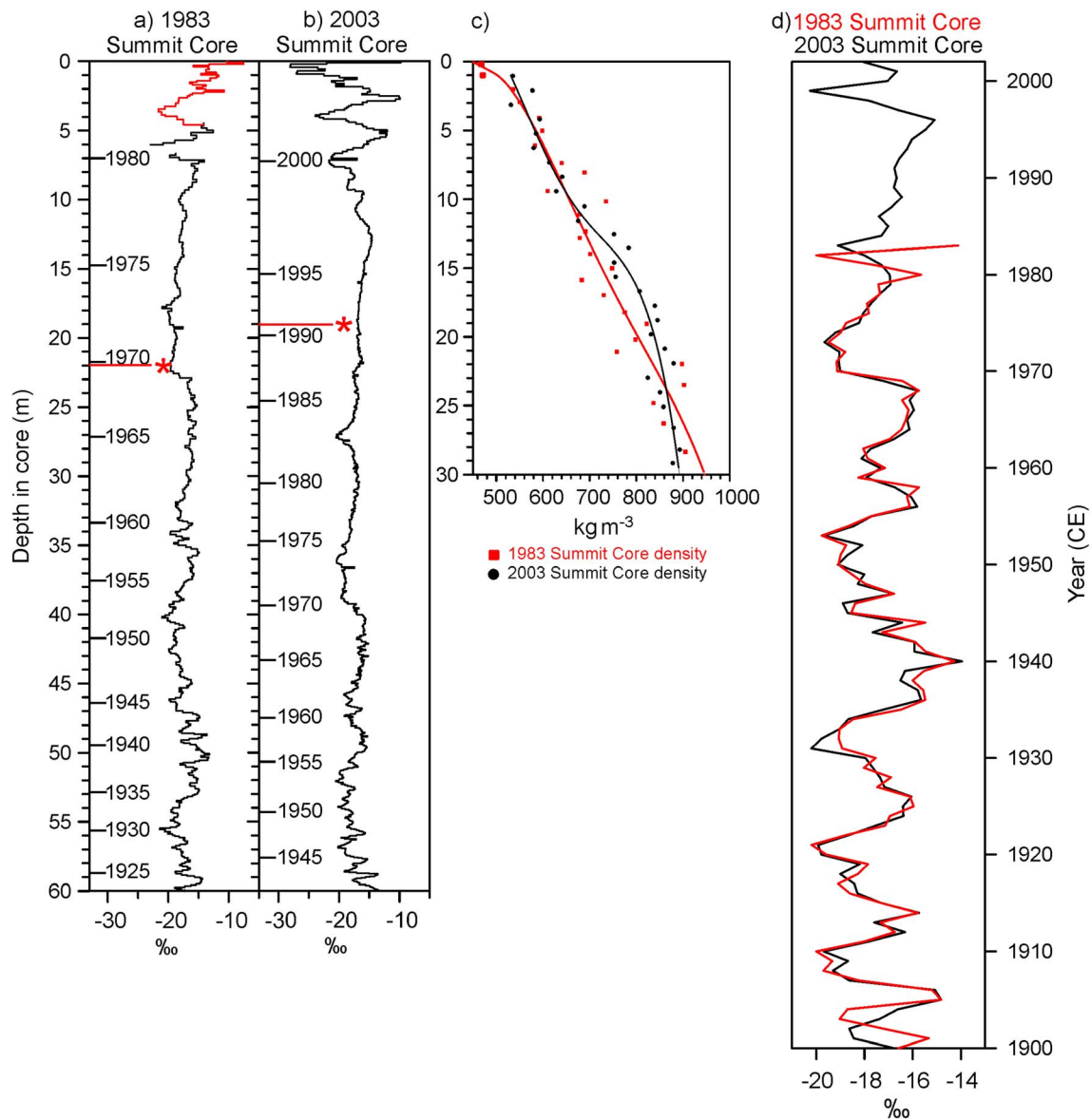


Figure 3. $\delta^{18}\text{O}$ stratigraphy in the top 60 m of (a) the 1983 QIC summit core (dated back to TY1925) topped by a 2.5 m pit and part of the summit shallow core (red curve) and (b) the 2003 QIC summit dome core (dated back to TY1945). The pore close-off density of 830 kg m^{-3} is marked by a red line and asterisk in each profile. (c) The density profiles to 30 m of both records are aligned by depth with the $\delta^{18}\text{O}$ plots. Each plot is overlain by a fourth-order regression curve. (d) Annual averages of $\delta^{18}\text{O}$ through the twentieth century for the 1983 (red curve) and the 2003 summit (black curve) cores.

free-standing water was encountered. In 2003, water accumulated in the bottom of the firn layer and ran into the borehole as the drilling continued below the firn/ice transition. So much water collected in the borehole that it had to be bailed out each morning before drilling could proceed. However, the $\delta^{18}\text{O}$ stratigraphic profiles of the pits and shallow cores (Figure S1 in the supporting information) indicate that the majority of the melt occurred before the deposition of each TY1 layer and percolated downward to collect above the top of the ice. This implies that mass was transferred, at least from 1983 to 2003, from the upper firn layers before the accumulation of the TY1 layer to the depth just above the firn/ice transition. However, despite the increase in postdepositional alteration of the $\delta^{18}\text{O}$ record, the annually averaged $\delta^{18}\text{O}$ time series from the two cores are highly reproducible where they overlap (Figure 3d).

3.1. The Effects of Recent El Niños on Peruvian Ice Fields

During the course of the expeditions to the Peruvian Andes since 1974 several strong El Niños occurred (1982/1983, 1986/1987, 1991/1992, 1997/1998, and 2015/2016, see Table S1 and the relevant text in the

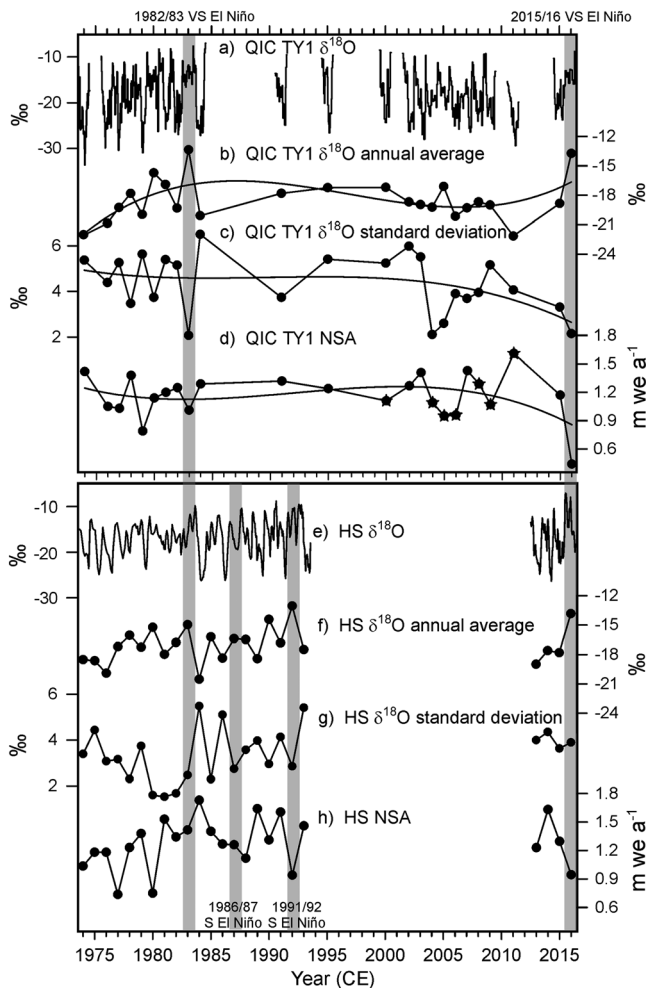


Figure 4. (a) Time series of the isotopic profiles of the most recent year (TY1) of firn/snow sampled during 24 expeditions over 43 years on the QIC (for years with multiple profiles only one is shown here), (b) annually averaged $\delta^{18}\text{O}$ of each QIC TY1 layer, (c) standard deviation of the $\delta^{18}\text{O}$ data for each QIC TY1 shown in Figure 4a, and (d) net sum of accumulation (NSA) in meters of water equivalent per year (mwe a^{-1}) on QIC. Years lacking density measurements are marked by stars and their NSA is derived using 450 kg m^{-3} , the average of the densities measured in the other 17 years. Third-order polynomial functions are shown for all 24 years (solid black lines). (e) $\delta^{18}\text{O}$ data from the Huascarán deep core are shown from 1973/1974 to 1992/1993 and from 2012/2013 to 2015/2016 as recorded in the 2016 shallow core, along with (f) $\delta^{18}\text{O}$ annual averages, (g) $\delta^{18}\text{O}$ standard deviation for each thermal year, and (h) NSA in mwe a^{-1} . Strong (S) ($2.0 > \text{ONI} > +1.0$) and very strong (VS) ($\text{ONI} > +2.0$) El Niños (Table S1) are marked by gray shading.

layers formed from a fraction of the meltwater have been observed at the boundaries of annual layers in the QIC (Thompson, 1980) and most recently in the stratigraphy of the 2016 summit pit (Figure S4 in the supporting information).

Without these strong El Niños, the QIC climate record would still be altered throughout the upper portion of the firn/ice column and its margins would still be in retreat, but it is apparent that these changes are greatly enhanced by these large intermittent events. For example, the 2015/2016 El Niño had easily observable consequences on a margin of the QIC where the decrease in surface area of the ice was $\sim 28\%$ greater than the average annual rate of decrease during the previous 15 years (Figure 5 and Table S2 in the supporting information), determined using ground-based observations (Figure S5 in supporting information) and satellite images.

supporting information). The QIC data set includes the very strong 1982/1983 El Niño (Oceanic Niño Index, or ONI $> +2.0$), and the deep core drilled in 1993 on HS includes the very strong 1982/1983 and strong 1986/1987 and 1991/1992 events (ONI $> +1.0$). The shallow core drilling conducted at both sites in July 2016 provides an excellent opportunity to examine the impact of the very strong 2015/2016 event. Unfortunately, no field program was conducted at either site in 1998 and 2010 so there are no data for the very strong 1997/1998 and the strong 2009/2010 El Niños.

Time series of TY1 parameters from the QIC summit and the annual averages from the HS col (Figure 4) demonstrate variations in $\delta^{18}\text{O}$ and NSA during strong El Niños with respect to nonevent years. The data from snow deposited within the TY1 layers provide the best record of $\delta^{18}\text{O}$ and NSA on the summit of the QIC (Figure S1 in the supporting information), as the original information about the atmospheric/oceanic processes that influence the snow isotopic chemistry is better preserved than in lower layers that have been altered by the recent post-depositional processes such as melting and water percolation in the austral spring subsequent to austral winter sampling. Representative profiles from each TY1 (where multiple profiles are available) are compiled into a composite time series which illustrates the characteristic $\delta^{18}\text{O}$ seasonality within each thermal year of snowfall (Figure 4a). The seasonal amplitudes, which range up to ~ 15 to 20‰ , are comparable with those in the Little Ice Age section of the 1983 and 2003 deep cores (Thompson et al., 1986, 2013). The time series of TY1 $\delta^{18}\text{O}$ averages (Figure 4b), standard deviations (SD), which represent the magnitudes of the seasonal variations (Figure 4c), and NSA (Figure 4d) are shown with third-order polynomial functions to illustrate decadal-scale variability. The annual values in Figures 4b–4d are averages of multiple pits excavated and/or shallow cores drilled in that year, where applicable. The very strong 1982/1983 and 2015/2016 El Niños are distinguished by annually averaged $\delta^{18}\text{O}$ values that are 5.6 and 5.2‰ (Figure 4b), respectively, above the mean for the non-El Niño years (-18.9‰). Their seasonal isotopic variations show little SASM depletion (Figures 4a and 4c) and are characterized by reduced NSA (Figure 4d) which may reflect low SASM precipitation but more likely is a result of high postdepositional ablation. Although the NSA of the 1982/1983 event is just 16% below the mean for the non-El Niño years ($1.2 \text{ meters water equivalent (mwe) a}^{-1}$), the upper limit of the NSA of the most recent El Niño is 64% below that mean. The 2015/2016 El Niño TY1 may have been altered by significant melting at the surface during the record warm austral summer in the vicinity of the QIC (Figure S3 in the supporting information) that preceded the 2016 field season which greatly contributed to the very low NSA for this year. Ice

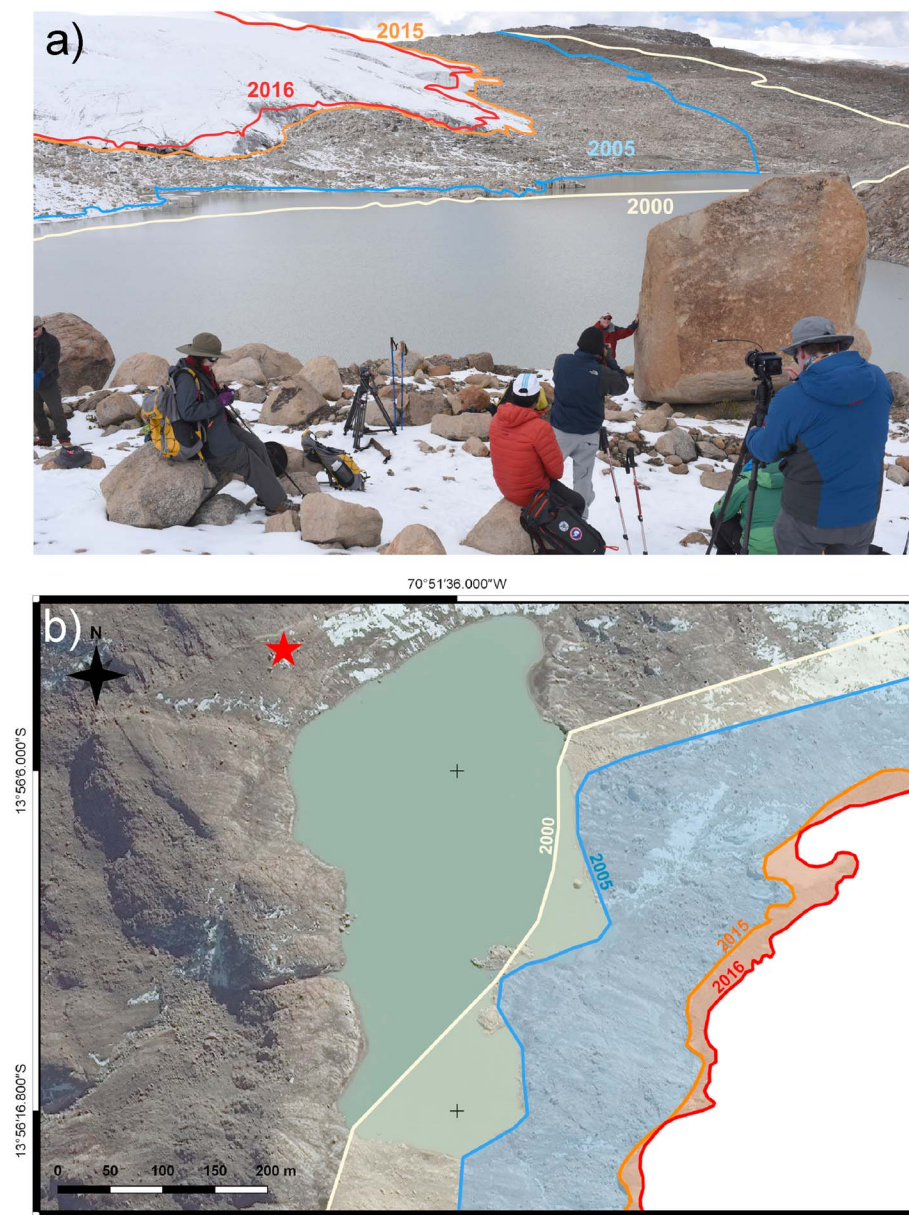


Figure 5. (a) Photograph taken along the western margin of the QIC in austral winter 2015 showing the position of the ice edge at that time. The positions of the ice margin in austral winters of 2000, 2005, and 2016 also are superimposed on the photograph. The original images (Figure S5 in the supporting information) were cropped and scaled using Adobe Photoshop CS6. (b) Satellite view of the ice margins composited from 2000 to 2005 terrestrial photographs and 2015 and 2016 satellite photographs from DigitalGlobe's WorldView-3. The position of the large boulder in Figure 5a is marked by the red star.

The Huascarán $\delta^{18}\text{O}$ data from TY 1973/1974 to 1992/1993 from the deep ice core drilled in 1993, along with data from the 2016 shallow core covering TY 2012/2013 to 2015/2016 (Figure 4e), demonstrate the preservation of the seasonal isotopic signal at this higher altitude site. Similar to El Niño characteristics in the QIC record, $\delta^{18}\text{O}$ annual averages for the 1991/1992 and 2015/2016 events are the highest of the record, with enrichments of 4.5‰ and 3.7‰, respectively, above the mean of the non-El Niño years (−17.5‰) (Figure 4f). The isotopic enrichment during the 1982/1983 El Niño is less remarkable (2.6‰) and the enrichment during the strong 1986/1987 El Niño is insignificant (1.2‰). None of the El Niños in the HS $\delta^{18}\text{O}$ record show SDs that are unique (Figure 4g). The 2015/2016 and 1991/1992 events are both marked by an NSA decrease of 28% compared to the non-El Niño mean (1.3 mwe a^{-1}). However, the 1986/1987 strong El Niño shows an insignificant NSA decrease of 3%, while the 1982/1983 NSA is anomalously positive (9%) with respect to the mean.

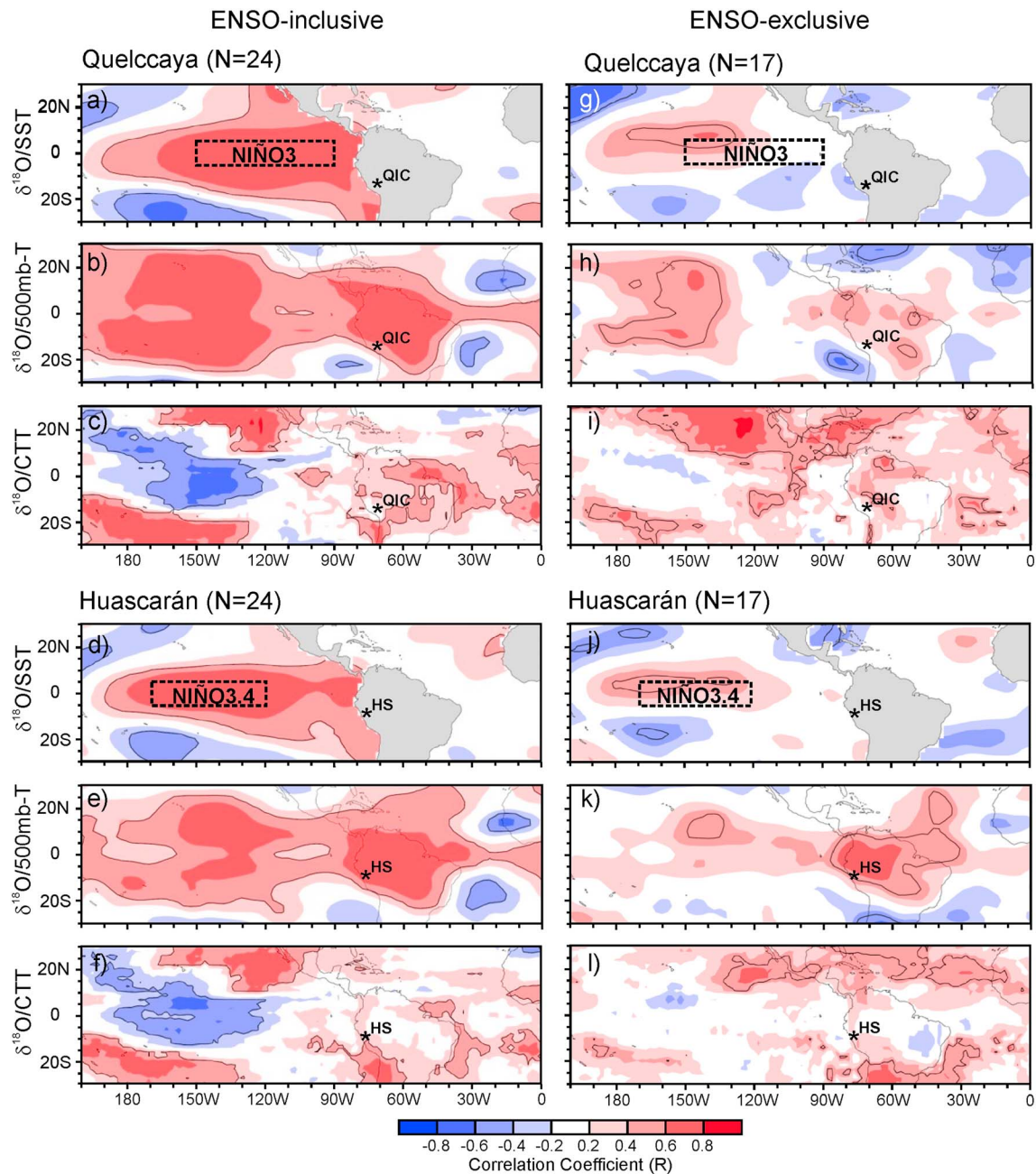


Figure 6. Pearson two-tailed correlation (R) fields between QIC TY1 $\delta^{18}\text{O}$ (between 1973/1974 and 2015/2016) and (a) DJF SSTs (Huang et al., 2015; Liu et al., 2015), (b) DJF 500 mb-T (Kalnay et al., 1996), and (c) DJF CTTs (Kalnay et al., 1996). (d–f) Same as in Figures 6a–6c but for HS TY $\delta^{18}\text{O}$ (1973/1974 to 1992/1993, 2012/2013 to 2015/2016). (g–i) Same as in Figures 6a–6c but with ENSO events of $-1.0 > \text{ONI} > +1.0$ excluded. (j–l) Same as for Figures 6d–6f but with ENSO events of $-1.0 > \text{ONI} > +1.0$ excluded. Red shading indicates positive R , blue shading indicates negative R , and black contours denote R values with significance levels (p) = 0.05.

4. Atmospheric/Oceanic Controls on QIC and HS $\delta^{18}\text{O}$ During Major ENSO Events

Hurley et al. (2015) found that precipitation amount on the QIC corresponds to regional atmospheric dynamics. Heavy snowfall events on the eastern Andes are associated with periods of high precipitation and low outgoing longwave radiation (OLR) over the western and central Amazon Basin. It has also been shown that stable isotopic ratios in Andean ice cores are closely related to tropical eastern Pacific sea surface temperatures (SSTs) (Bradley et al., 2003; Thompson et al., 2011, 2013). Henderson et al. (1999) correlated $\delta^{18}\text{O}$ in HS ice with 500 millibar (mb) zonal wind variations over tropical South America, which they

speculated may be related to atmospheric temperatures and precipitation variations. Thus, the isotopic chemistry of the precipitation in the tropical Andes in general, and on the QIC and HS in particular, is controlled by both atmospheric/oceanic processes to the west and atmospheric processes to the east.

Figure 6 illustrates the spatial correlation (R) fields between tropical western hemisphere oceanic and atmospheric conditions during the SASM from December to February (DJF) and all the QIC TY1 and HS annual averages of $\delta^{18}\text{O}$ (Figures 4b and 4f). The QIC and HS R fields (Figures 6a and 6b, and 6d and 6e, respectively) display ENSO-type patterns; specifically, isotopic values in SASM snow are positively and significantly correlated with tropical eastern Pacific SSTs, and with midtroposphere temperatures (500 mb-T) from the central Pacific eastward over tropical South America to western Africa. The region of most significant QIC $\delta^{18}\text{O}/\text{SST}$ correlation is located within the NIÑO3 region (Figure 6a), while the area of most significant HS $\delta^{18}\text{O}/\text{SST}$ correlation coincides with NIÑO3.4 (Figure 6d). Regions of significant correlations between $\delta^{18}\text{O}$ and cloud top temperatures (CTT) overlie the $\delta^{18}\text{O}/\text{SST}$ R fields (Figures 6c, 6f), such that less (more) negative TY1 $\delta^{18}\text{O}$ values occur with higher (lower) Niño index region SSTs and stronger (weaker) convection characterized by lower (higher) cloud top temperatures. When the strong and very strong warm ("El Niño") and cold ("La Niña") ENSO events, as defined by the ONI (Table S1 in the supporting information), are removed from the calculations, the large and statistically significant R fields for the tropical Pacific SSTs and overlying midtroposphere temperatures (Figures 6g and 6h for QIC; Figures 6j and 6k for HS) substantially weaken. The QIC and HS $\delta^{18}\text{O}/\text{SST}$ R fields contract and shift northwest of the centers of NIÑO3 and NIÑO3.4, respectively. In the absence of these ENSO events statistically significant negative correlations between $\delta^{18}\text{O}$ and CTTs over the Pacific also diminish dramatically (Figure 6i for QIC and Figure 6l for HS).

Although the ocean/atmosphere teleconnections respond more or less similarly for both the QIC and HS in the tropical Pacific in ENSO-inclusive and exclusive scenarios, the differences in midtropospheric relationships with $\delta^{18}\text{O}$ are more pronounced over northern South America for the QIC. Enriched (depleted) QIC $\delta^{18}\text{O}$ is associated with significant tropical atmospheric warmth (cooling) at the 500 mb level throughout the Western Hemisphere (Figure 6b), but almost all the significant correlation fields disappear in the absence of major ENSOs (Figure 6h). QIC $\delta^{18}\text{O}/\text{CTT}$ correlations are positive in NE South America (Figure 6c), but without the presence of ENSO conditions significant R fields are absent (Figure 6i). In contrast, significant HS $\delta^{18}\text{O}/500$ mb-T R fields that occur from the tropical Atlantic to the Andes in the El Niño-inclusive scenario (Figure 6e) persist, although are weaker, in the ENSO exclusive case (Figure 6k). Little significant HS $\delta^{18}\text{O}/\text{CTT}$ correlation exists over the Amazon Basin or the Peruvian Andes in either scenario (Figures 6f and 6l).

5. Discussion

On interannual time scales the SASM and ENSO (as defined by the NIÑO3.4 index) are significantly correlated (Vuille & Werner, 2005). By extension $\delta^{18}\text{O}$ and the SASM are also linked, since ENSO exerts some influence on $\delta^{18}\text{O}$ in these ice fields. This is observationally and statistically evident for the QIC (Figures 6a and S6a in the supporting information), but statistically less so for HS (Figures 6d and S6b in the supporting information). QIC and HS $\delta^{18}\text{O}/500$ mb-T are similar to the SST/ $\delta^{18}\text{O}$ relationships to the extent that the R fields in the ENSO-exclusive scenarios are smaller and less significant than in the ENSO-inclusive cases (Figures 6h and 6b and Figures 6k and 6e, respectively), and the tests for significance differences show more ENSO influence on QIC than on HS $\delta^{18}\text{O}/500$ mb-T correlations (Figures S6c and S6d in the supporting information). The differences are localized in the tropical Pacific for both ice fields and in the Caribbean and tropical North Atlantic for the QIC. For HS $\delta^{18}\text{O}/\text{SST}$ and 500 mb-T, the smaller statistical differences between ENSO-inclusive and exclusive scenarios may indicate that while ENSO has minor influence on temperature-linked variations in $\delta^{18}\text{O}$, these relationships are consistent regardless of the presence or absence of strong ENSO conditions.

Linkages between CTTs, deep convection, and the isotopic composition of precipitation have been noted in several tropical regions. Cai and Tian (2016) demonstrated statistically that the isotopic composition of precipitation in the East Asian Monsoon region is correlated with convective intensity during the summer monsoon, and thus related to cloud top height. Monthly $\delta^{18}\text{O}$ in precipitation in Hong Kong from 1984 to 2009 was significantly correlated ($p < 0.01$) with convective cloud top pressure (CTP) and CTT. For CTP this

correlation was valid over regional scales in areas of monsoon activity and demonstrated that wet season $\delta^{18}\text{O}$ is largely influenced by large-scale atmospheric circulation. Scholl et al. (2009) found a correlation between $\delta^{18}\text{O}$ in rain over Puerto Rico and echo top altitude and explained this in part through the control of condensation temperature on stable isotopic composition. In Papua, Indonesia, rainfall $\delta^{18}\text{O}$ variability on a variety of timescales is controlled by regional convection and mean condensation levels and, by implication, temperatures (Permana et al., 2016).

The ENSO influence of the tropical Pacific $\delta^{18}\text{O}/\text{SST}$ and $\delta^{18}\text{O}/500\text{ mb-T}$ linkages are more relevant for the QIC than for HS, as demonstrated by differences between z scores of the ENSO-inclusive and ENSO-exclusive scenarios (Figures S6a–S6d in the supporting information). Likewise, the contribution of the ENSO years to the correlation of $\delta^{18}\text{O}$ in snowfall with CTT over the central tropical Pacific (Figure 6c) is more significant for the QIC (Figures S6e and S6f, supporting information). Significant positive QIC $\delta^{18}\text{O}/\text{CTT}$ correlations occur over the northern and eastern Amazon Basin, upwind of the QIC, and the central Andes (Figure 6c). The positive correlations indicate that more isotopically depleted (enriched) QIC summer snow is associated with lower (higher) cloud top temperatures, suggesting that condensation occurs at colder (warmer), higher (lower) elevations. Thus, just as in the East Asian Monsoon system (Cai & Tian, 2016), the stable isotopic chemistry of the precipitation from the SASM is also apparently affected by large-scale upper atmospheric circulation, which is consistent with the results of Hurley et al. (2015). Samuels-Crow et al. (2014) found that stable isotopes in vapor (specifically δD) en route to the central tropical Andes are strongly affected by convection, and that the isotopic values that are lower than predicted by Rayleigh distillation at a given water vapor concentration are associated with low OLR values. When ENSO events are removed, the fields of significant correlation between QIC $\delta^{18}\text{O}$ and convective CTTs almost completely disappear over the Amazon Basin (Figure 6i). By observation, this might suggest that ENSO is an important driver in the QIC $\delta^{18}\text{O}/\text{CTT}$ relationship; however, statistically the differences do not appear to be significant in this region (Figure S6e in the supporting information), although during an El Niño higher SSTs in the eastern tropical Pacific inhibit convection over the tropical Andes by shifting and weakening the Walker circulation (Garreaud & Aceituno, 2001; Vuille et al., 2000) and by enhancing the upper-level westerly air flow while impeding the moisture-bearing easterlies.

Significant interannual correlations have been demonstrated between midtropospheric temperatures and the net balance on the Chacaltaya glacier on the Bolivian Altiplano (Francou et al., 2003). Precipitation on the Altiplano is linked to zonal winds such that westerlies (easterlies) are associated with low (high) precipitation anomalies. This zonal pattern is affected by fluctuations in meridional baroclinicity, which is in turn driven by the gradient in upper tropospheric temperature anomalies (Garreaud & Aceituno, 2001). The differences between QIC ENSO-inclusive and exclusive scenarios imply that during an El Niño, the strengthening of the positive QIC $\delta^{18}\text{O}/500\text{ mb-T}$ R fields (Figure 6b) enhances the westerly air flow that diminishes SASM deep convection, resulting in ^{18}O enrichment of the snow that falls on the ice cap (Figure 6c). The opposite scenario occurs during a La Niña. However, the HS $\delta^{18}\text{O}/500\text{ mb-T}$ R fields over northern South America and (to a lesser extent) over the eastern tropical Pacific persist regardless of the presence of ENSO (Figures 6e and 6k). Thus, it is possible that the effects of fluctuations in the zonal circulation caused by changes in the meridional baroclinicity during ENSO do not exert the same influences over HS in the Cordillera Blanca (CB) in northern Peru as they do over the QIC in southern Peru.

The link between ENSO and glacier mass balance in the CB is similar to that on the Altiplano, but the conditions that govern this relationship oscillate latitudinally along the axis of the tropical Andes (Vuille, Kaser, et al., 2008). ENSO appears to exert a more consistent, stable, and uniform effect on the Altiplano region, whereas the CB may be more susceptible to decadal scale changes in the tropical Pacific SSTs in response to the regional patterns of upper-level zonal winds. The upper tropospheric flow that drives the easterly moisture influx which is pronounced over the Altiplano does not appear to influence precipitation in the CB in a uniform and consistent way during all El Niño years. This is suggested by the anomalously higher NSA on HS during the very strong 1982/1983 El Niño. The CB may mark the northern boundary of this temperature-driven upper air zonal circulation. However, before the mid-1970s the correlation between glacier mass balance in the CB and NIÑO3.4 SST was much more significant than after (Vuille, Kaser, et al., 2008), suggesting that the reorganization of Pacific Ocean SSTs during the mid-1970s (Mantua et al., 1997) may have affected the latitudinal position of the upper-level westerlies over the Andes. This may also be

the case for the relationships between ENSO indicators and HS $\delta^{18}\text{O}$, which is driven by the same tropical oceanic and atmospheric processes that govern glacier mass balance.

6. Summary and Conclusions

The recent changes in the surface layers of the Quelccaya ice cap result primarily from tropospheric warming over the highest elevations of the tropical Andes which has been well documented over recent decades (Vuille et al., 2015). Model results predict warming over this region in the 21st century (Urrutia & Vuille, 2009), although the greater warming will occur in the winter. Indeed, there is extensive evidence that this has been responsible for the dramatic retreat of the Quelccaya margins and the eradication of the climate signal in the top of the deep ice cores drilled in 2003 (Thompson et al., 2006, 2013). This collection of shallow and deep cores drilled since 1974 illustrates the progression of this phenomenon over the last four decades. Moreover, they emphasize the one advantage of the $\delta^{18}\text{O}$ data analyzed from relatively fresh snow collected in pits and shallow cores over the past 43 years relative to the more postdepositionally modified $\delta^{18}\text{O}$ data from the upper sections of the deep ice cores. Fortunately, the seasonal isotopic signal on Huascarán is still preserved, and perhaps because of its higher elevation, the freezing level height has not as yet risen to the level of its col from where the cores were recovered.

Monitoring of the QIC over the last 43 years demonstrates that the seasonal signal of $\delta^{18}\text{O}$ has rapidly attenuated since the beginning of the 21st century, particularly below the top few meters of firn, most likely due to melting and percolation. However, during the 2015/2016 El Niño the isotopic seasonality was greatly diminished, as it was in 1982/1983. Similar to the conditions on the QIC, on HS the 1991/1992 and 2015/2016 events are also characterized by ^{18}O enrichment and NSA decrease, although these characteristics are not apparent in the 1982/1983 and 1986/1987 El Niños. These trends are indicative of increases in surface temperatures which enhance vapor diffusion through the upper layers of the firn. This tends to smooth the seasonal variations of stable isotopes through the firn in the lower elevation QIC, although the 2015/2016 TY1 may have been affected by melt.

The interannual $\delta^{18}\text{O}$ values of the precipitation that falls on both the QIC and HS are influenced by sea surface temperatures and, to a lesser extent, regional-scale variations in the tropospheric temperatures over the tropical Pacific Ocean and the northern Amazon Basin. ENSO appears to have a more consistent and uniform effect on the southern Peru/Altiplano region than on the Cordillera Blanca, which may be more susceptible to decadal scale changes in the tropical Pacific SSTs via the regional patterns of upper-level zonal winds. Significant correlations between interannual QIC $\delta^{18}\text{O}$ and high cloud top temperatures suggest a link between stable isotopes in precipitation and temperature (and thus altitude) during condensation in convective clouds over the northern Amazon Basin and along the eastern flanks of the Andes. These relationships add to earlier research indicating that the isotopic chemistry in Andean precipitation is strongly influenced not only from the east (Grootes et al., 1989; Henderson et al., 1999; Hurley et al., 2015) but also by perturbations in the Walker circulation during ENSO events that in turn are affected by oceanic processes (Thompson et al., 2013; Vuille et al., 2003; Vuille & Werner, 2005).

The warming that has occurred in the tropical Andes since the middle of the twentieth century has had marked consequences for the glaciers in the region. Mean annual surface temperatures in the central Andes and free air temperatures at 500 mb have been rising contemporaneously over this period (Salzmann et al., 2013) as the 0°C isotherm has lifted (Bradley et al., 2009). This has been exacerbated by the effects of major El Niños, and the most recent event has had effects on the QIC that are greater than those in 1982/1983. Evidence indicates that the most recent event has, at least temporarily, accelerated the rate of retreat of the QIC and of the obliteration of the climate record stored in the ice. This isotopic smoothing is not observed in the Little Ice Age (~1550 to ~1880 C.E.) portion of the deep QIC ice cores (Thompson et al., 1986, 2013), in part because the 0°C isotherm was positioned far below the summit during that period, which is currently the case for higher-altitude ice fields such as Huascarán where the seasonal isotopic variations have not changed since the LIA (Thompson, 2000). While the oxygen isotopic record from the firn core recovered from the col of Huascarán in 2016 at 6,050 m still preserves a largely unaltered deposition signal, it is only a matter of time before this higher-elevation record will be similarly compromised by the ongoing warming. It is possible that the warming trend of the regional climate is near or at a threshold beyond which additional warming from very strong El Niños like the 2015/2016 event, along with elevated freezing levels and

feedbacks such as reduced snow cover, will augment the ice loss on even the highest-elevation Peruvian glaciers in the coming decades.

Acknowledgments

Funding for the 2016 field project and the 2013 drilling project was provided by The National Science Foundation (NSF) Paleoclimate Program awards RAPID AGS-1603377 and AGS-0823586, respectively and by the Ohio State University (OSU). Prior field projects back to 1974 were funded by multiple awards from NSF, NOAA, and OSU. The authors thank three anonymous reviewers for their suggestions and comments which greatly improved the quality of this paper. We thank all the field and laboratory team members, many from the Byrd Polar and Climate Research Center, who have worked so diligently over the years to acquire these snow pit samples and firn/ice cores and to extract their preserved climate histories. We thank J. P. Nicolas (OSU) for contributing satellite views of QIC ice margin and calculations of ice margin retreat with support from NSF award PLR-1612741. We acknowledge the efforts of our Peruvian colleagues from the Servicio Nacional de Meteorología e Hidrología, B. Morales Arnao, C. Portocarrero, Instituto Nacional de Investigación en Glaciares y Ecosistemas de Montaña, and our mountaineers, led by B. Vicencio, who cooperated with us to make all the field programs over the last four decades possible. This is Byrd Polar Climate and Research Center contribution number C-1571. The data, including all isotopic sample measurements presented in this study, are archived at the National Oceanic and Atmospheric Administration World Data Center-A for Paleoclimatology: <https://www.ncdc.noaa.gov/paleo/study/22251>.

References

- Albert, T., Klein, A., Kincaid, J. L., Huggel, C., Racoviteanu, A. E., Arnaud, Y., ... Ceballos, J. L. (2014). Remote sensing of rapidly diminishing tropical glaciers in the northern Andes. In J. S. Kargel, G. J. Leonard, M. P. Bishop, A. Kääh, & B. H. Raup (Eds.), *Global land ice measurements from space* (pp. 609–638). Berlin Heidelberg: Springer.
- Bradley, R. S., Keimig, F. T., Diaz, H. F., & Hardy, D. R. (2009). Recent changes in freezing level heights in the Tropics with implications for the deglaciation of high mountain regions. *Geophysical Research Letters*, *36*, L17701. <https://doi.org/10.1029/2009GL037712>
- Bradley, R. S., Vuille, M., Diaz, H. F., & Vergara, W. (2006). Threats to water supplies in the tropical Andes. *Science*, *312*, 1755–1756. <https://doi.org/10.1126/science.1128087>
- Bradley, R. S., Vuille, M., Hardy, D., & Thompson, L. G. (2003). Low latitude ice cores record Pacific sea surface temperatures. *Geophysical Research Letters*, *30*(4), 1174. <https://doi.org/10.1029/2002GL016546>
- Brecher, H. H., & Thompson, L. G. (1993). Measurement of the retreat of Qori Kalis glacier in the tropical Andes of Peru by terrestrial photogrammetry. *Photogrammetric Engineering and Remote Sensing*, *59*, 1017–1022.
- Cai, Z., & Tian, L. (2016). Atmospheric controls on seasonal and interannual variations in the precipitation isotope in the East Asian Monsoon region. *Journal of Climate*, *29*, 1339–1352. <https://doi.org/10.1029/2015JD023323>
- Dansgaard, W. (1964). Stable isotopes in precipitation. *Tellus*, *16*, 436–468. <https://doi.org/10.3402/tellusa.v16i4.8993>
- Diaz, H. F., Bradley, R. S., & Ning, L. (2014). Climatic changes in mountain regions of the American Cordillera and the Tropics: Historical changes and future outlook. *Arctic, Antarctic, and Alpine Research*, *46*(4), 735–743. <https://doi.org/10.1657/1938-4246-46.4.735>
- Franco, B., Vuille, M., Wagnon, P., Mendoza, J., & Sicart, J.-E. (2003). Tropical climate change recorded by a glacier in the central Andes during the last decades of the twentieth century: Chacaltaya, Bolivia, 16°S. *Journal of Geophysical Research*, *108*(D5), 4154. <https://doi.org/10.1029/2002JD002959>
- Garreaud, R., & Aceituno, P. (2001). Interannual rainfall variability over the South American Altiplano. *Journal of Climate*, *14*, 2779–2789. <https://doi.org/10.1029/2000JD001187>
- Garreaud, R., Vuille, M., & Clement, A. C. (2003). The climate of the Altiplano: observed current conditions and mechanisms of past changes. *Palaeogeography Palaeoclimatology Palaeoecology*, *194*, 5–22. [https://doi.org/10.1016/S0031-0182\(03\)00269-4](https://doi.org/10.1016/S0031-0182(03)00269-4)
- Garreaud, R. D., Vuille, M., Compagnucci, R., & Marengo, J. (2009). Present-day South American climate. *Palaeogeography Palaeoclimatology Palaeoecology*, *281*, 180–195. <https://doi.org/10.1016/j.palaeo.2007.10.032>
- Groote, P. M., Stuvier, M., Thompson, L. G., & Mosley-Thompson, E. (1989). Oxygen isotope changes in tropical ice, Quelccaya, Peru. *Journal of Geophysical Research*, *94*(D1), 1187–1194. <https://doi.org/10.1029/JD094iD01p01187>
- Hanshaw, M. N., & Bookhagen, B. (2014). Glacial areas, lake areas, and snow lines from 1975 to 2012: status of the Cordillera Vilcanota, including the Quelccaya Ice Cap, northern central Andes, Peru. *The Cryosphere*, *8*, 359–376. <https://doi.org/10.5194/tc-8-359-2014>
- Henderson, K. A., Thompson, L. G., & Lin, P.-N. (1999). Recording of El Niño in ice core $\delta^{18}\text{O}$ records from Nevado Huascarán, Peru. *Journal of Geophysical Research*, *104*(D24), 31,053–31,065.
- Huang, B., Banzon, V. F., Freeman, E., Lawrimore, J., Liu, W., Peterson, T. C., ... Zhang, H.-M. (2015). Extended reconstructed sea surface temperature version 4 (ERSST.v4). Part I: Upgrades and intercomparisons. *Journal of Climate*, *28*, 911–930. <https://doi.org/10.1029/2015JD023323>
- Hurley, J. V., Vuille, M., Hardy, D. R., Burns, S. J., & Thompson, L. G. (2015). Cold air incursions, $\delta^{18}\text{O}$ variability, and monsoon dynamics associated with snow days at Quelccaya Ice Cap, Peru. *Journal of Geophysical Research: Atmospheres*, *120*, 7467–7487. <https://doi.org/10.1002/2015JD023323>
- Johnsen, S. J., Clausen, H. B., Cuffey, K. M., Hoffmann, G., Schwander, J., & Creyts, T. (2000). Diffusion of stable isotopes in polar firn and ice: the isotope effect in firn diffusion. In T. Hondoh (Ed.), *Physics of ice core records* (pp. 121–140). Sapporo, Japan: Hokkaido University Press.
- Kalnay, E., Kanamitsu, M., Kistler, R., Collins, W., Deaven, D., Gandin, L., ... Joseph, D. (1996). The NCEP/NCAR 40-year reanalysis project. *Bulletin of the American Meteorological Society*, *77*(3), 437–471. <https://doi.org/10.1029/1996JG000927>
- Lenters, J. D., & Cook, K. H. (1997). On the origin of the Bolivian High and related circulation features of the South American climate. *Journal of the Atmospheric Sciences*, *54*, 656–677. <https://doi.org/10.1029/1997JD009410>
- Liu, W., Huang, B., Thorne, P. W., Banzon, V. F., Zhang, H.-M., Freeman, E., ... Woodruff, S. D. (2015). Extended reconstructed sea surface temperature version 4 (ERSST.v4): Part II. Parametric and structural uncertainty estimations. *Journal of Climate*, *28*, 931–951. <https://doi.org/10.1029/2015JD023323>
- Mantas, V. M., Liu, Z., Caro, C., & Pereira, A. J. S. C. (2015). Validation of TRMM multi-satellite precipitation analysis (TMPA) products in the Peruvian Andes. *Atmospheric Research*, *163*, 132–145. <https://doi.org/10.1016/j.atmosres.2014.11.012>
- Mantua, N. J., Hare, S. R., Zhang, Y., Wallace, J. M., & Francis, R. C. (1997). A Pacific interdecadal climate oscillation with impacts on salmon production. *Bulletin of the American Meteorological Society*, *78*(6), 1069–1079. <https://doi.org/10.1029/1997JD001069>
- Pepin, N., Bradley, R. S., Diaz, H. F., Baraer, M., Caceres, E. B., Forsythe, N., ... Yang, D. Q. (2015). Elevation-dependent warming in mountain regions of the world. *Nature Climate Change*, *5*, 424–430. <https://doi.org/10.1038/nclimate2563>
- Permana, D. S., Thompson, L. G., & Setyadi, G. (2016). Tropical West Pacific moisture dynamics and climate controls on rainfall isotopic ratios in southern Papua, Indonesia. *Journal of Geophysical Research: Atmospheres*, *121*, 2222–2245. <https://doi.org/10.1029/2015JD023893>
- Perry, L. B., Seimon, A., & Kelly, G. M. (2014). Precipitation delivery in the tropical high Andes of southern Peru: New findings and paleoclimatic implications. *International Journal of Climatology*, *34*, 197–215. <https://doi.org/10.1002/joc.3679>
- Rabatel, A., Franco, B., Soruco, A., Gomez, J., Cáceres, B., Ceballos, J. L., ... Wagnon, P. (2013). Current state of glaciers in the tropical Andes: A multi-century perspective on glacier evolution and climate change. *The Cryosphere*, *7*(1), 81–102. <https://doi.org/10.5194/tc-7-81-2013>
- Rozanski, K., Araguás-Araguás, L., & Gonfiantini, R. (1993). Isotopic patterns in modern global precipitation, In edited P. K. Swart et al. (Eds.), *Climate change in continental isotopic records, Geophysical Monograph Series*, (Vol. 78, pp. 1–36). Washington, DC: American Geophysical Union.
- Salzmann, N., Huggel, C., Rohrer, M., Silverio, W., Mark, B. G., Burns, P., & Portocarrero, C. (2013). Glacier changes and climate trends derived from multiple sources in the data scarce Cordillera Vilcanota region, southern Peruvian Andes. *The Cryosphere*, *7*, 103–118. <https://doi.org/10.5194/tc-7-103-2013>

- Samuels-Crow, K. E., Galewsky, J., Hardy, D. R., Sharp, Z. D., Worden, J., & Braun, C. (2014). Upwind convective influences on the isotopic composition of atmospheric water vapor over the tropical Andes. *Journal of Geophysical Research: Atmospheres*, *119*, 7051–7063. <https://doi.org/10.1002/2014JD021487>
- Schauwecker, S., Rohrer, M., Acuña, D., Cochachin, A., Dávila, L., Frey, H., ... Vuille, M. (2014). Climate trends and glacier retreat in the Cordillera Blanca, Peru, revisited. *Global and Planetary Change*, *119*, 85–97. <https://doi.org/10.1016/j.gloplacha.2014.05.005>
- Scholl, M. A., Shanley, J. B., Zegarra, J. P., & Coplen, T. B. (2009). The stable isotope amount effect: New insights from NEXRAD echo tops, Luquillo Mountains, Puerto Rico. *Water Resources Research*, *45*, W12407. <https://doi.org/10.1029/2008WR007515>
- Stichler, W., Schotterer, U., Fröhlich, K., Ginot, P., Kull, C., Gäggeler, H., & Pouyaud, B. (2001). Influence of sublimation on stable isotope records recovered from high-altitude glaciers in the tropical Andes. *Journal of Geophysical Research*, *106*, 22,613–22,620.
- Stroup, J. S., Kelly, M. A., Lowell, T. V., Applegate, P. J., & Howley, J. A. (2014). Late Holocene fluctuations of Qori Kalis outlet glacier, Quelccaya ice cap, Peruvian Andes. *Geology*, *42*(4), 347–350. <https://doi.org/10.1130/G35245.1>
- Thompson, L. G. (1980). Glaciological investigations of the tropical Quelccaya ice cap, Peru. *Journal of Glaciology*, *25*(91), 69–84.
- Thompson, L. G. (2000). Ice core evidence for climate change in the Tropics: implications for our future. *Quaternary Science Reviews*, *19*, 19–35.
- Thompson, L. G., Bolzan, J. F., Brecher, H. H., Kruss, P. D., Mosley-Thompson, E., & Jezek, K. C. (1982). Geophysical investigations of the tropical Quelccaya ice cap, Peru. *Journal of Glaciology*, *28*(98), 57–69.
- Thompson, L. G., Mosley-Thompson, E., Bolzan, J. F., & Koci, B. R. (1985). A 1500-year record of tropical precipitation in ice cores from the Quelccaya ice cap, Peru. *Science*, *229*, 971–973. <https://doi.org/10.1126/science.229.4717.971>
- Thompson, L. G., Mosley-Thompson, E., Brecher, H., Davis, M., Leon, B., Les, D., ... Mountain, K. (2006). Abrupt tropical climate change: Past and present. *Proceedings of the National Academy of Sciences of the United States of America*, *103*(28), 10,536–10,543. <https://doi.org/10.1073/pnas.0603900103>
- Thompson, L. G., Mosley-Thompson, E., Dansgaard, W., & Grootes, P. M. (1986). The Little Ice age as recorded in the stratigraphy of the tropical Quelccaya ice cap. *Science*, *234*, 361–364. <https://doi.org/10.1126/science.234.4774.361>
- Thompson, L. G., Mosley-Thompson, E., Davis, M. E., & Brecher, H. H. (2011). Tropical glaciers, recorders and indicators of climate change, are disappearing globally. *Annals of Glaciology*, *52*(59), 23–34. <https://doi.org/10.3189/172756411799096231>
- Thompson, L. G., Mosley-Thompson, E., Davis, M. E., Lin, P.-N., Henderson, K. A., Cole-Dai, J., ... Liu, K.-b. (1995). Late Glacial Stage and Holocene tropical ice core records from Huascarán, Peru. *Science*, *269*, 46–50. <https://doi.org/10.1126/science.269.5220.46>
- Thompson, L. G., Mosley-Thompson, E., Davis, M., Lin, P.-N., Yao, T., Dyurgerov, M., & Dai, J. (1993). "Recent warming": Ice core evidence from tropical ice cores with emphasis upon Central Asia. *Global and Planetary Change*, *7*, 145–156.
- Thompson, L. G., Mosley-Thompson, E., Davis, M. E., Zagorodnov, V. S., Howat, I. M., Mikhalenko, V. N., & Lin, P.-N. (2013). Annually resolved ice core records of tropical climate variability over the past ~1800 years. *Science*, *340*, 945–950. <https://doi.org/10.1126/science.1234210>
- Urrutia, R., & Vuille, M. (2009). Climate change projections for the tropical Andes using a regional climate model: Temperature and precipitation simulations for the end of the 21st century. *Journal of Geophysical Research*, *114*, D02108. <https://doi.org/10.1029/2008JD011021>
- Vuille, M., Bradley, R. S., & Keimig, F. (2000). Interannual climate variability in the Central Andes and its relation to tropical Pacific and Atlantic forcing. *Journal of Geophysical Research*, *105*(D10), 12,447–12,460. <https://doi.org/10.1029/2000JD900134>
- Vuille, M., Bradley, R. S., Werner, M., Healy, R., & Keimig, F. (2003). Modeling $\delta^{18}\text{O}$ in precipitation over the tropical Americas: 1. Interannual variability and climatic controls. *Journal of Geophysical Research*, *108*(D6), 4174. <https://doi.org/10.1029/2001JD002038>
- Vuille, M., Francou, B., Wagnon, P., Juen, I., Kaser, G., Mark, B. G., & Bradley, R. S. (2008). Climate change and tropical Andean glaciers: Past, present and future. *Earth Science Reviews*, *89*, 79–96. <https://doi.org/10.1016/j.earscirev.2008.04.002>
- Vuille, M., Franquist, E., Garreaud, R., Lavado Casimiro, W. S., & Cáceres, B. (2015). Impact of the global warming hiatus on Andean temperature. *Journal of Geophysical Research: Atmospheres*, *120*, 3745–3757. <https://doi.org/10.1002/2015JD023126>
- Vuille, M., Kaser, G., & Juen, I. (2008). Glacier mass balance variability in the Cordillera Blanca, Peru and its relationship with climate and large-scale circulation. *Global and Planetary Change*, *62*, 14–28. <https://doi.org/10.1016/j.gloplacha.2007.11.003>
- Vuille, M., & Werner, M. (2005). Stable isotopes in precipitation recording South American summer monsoon and ENSO variability: Observations and model results. *Climate Dynamics*, *25*, 401–413. <https://doi.org/10.1007/s00382-005-0049-9>